Received: 14 April 2016 | Revised: 21 June 2016 | Accepted: 29 June 2016

DOI 10.1002/bip.22913

ORIGINAL ARTICLE

WILEY PeptideScience

Insights into peptide-membrane interactions of newly synthesized, nitroxide-containing analogs of the peptaibiotic trichogin GA IV using EPR

Marco Bortolus*[1] | Annalisa Dalzini[1] | Anna Lisa Maniero[1] | Giacomo Panighel[1] | Alvaro Siano[1,2] | Claudio Toniolo[1,3] | Marta De Zotti*[1] | Fernando Formaggio[1,3]

[1] Department of Chemistry, University of Padova, Padova, 35131, Italy

[2] Departamento de Química Orgánica, Facultad de Bioquímica y Ciencias Biológicas (FBCB), Universidad Nacional del Litoral (UNL), 3000 Santa Fe, Argentina

[3] Institute of Biomolecular Chemistry, Padova Unit, CNR, Padova, 35131, Italy

Correspondence
Fernando Formaggio, Department of Chemistry, University of Padova, via Marzolo 1, 35131 Padova, Italy.
Email: fernando.formaggio@unipd.it

Funding Information
This work was supported by Fondazione CARIPARO (Progetti Eccellenza 2011/2012) and the Italian Ministry of University and Research (MIUR) through PRIN 2010-2011 (prot. 2010NRREPL) and Futuro in Ricerca 2013 (grant n. RBFR13RQXM, to M.D.Z.).

*M.B. and M.D.Z. both authors contributed equally.

Abstract

Trichogin GA IV is a short-length (10-amino acid long), mostly hydrophobic, peptaibiotic with an N-terminal fatty acyl chain and a C-terminal 1,2-amino alcohol. A cardinal role of the terminal moieties in the cytotoxic activity of trichogin has been recently found. Previously, peptide orientation and dynamics of trichogin analogs in the membrane were studied using methyl ester derivatives. Therefore, in the present work we synthesized several trichogin analogs with naturally occurring terminal groups to verify whether these moieties have any effect on peptide-membrane interaction. These trichogin analogs, both neutral and carrying a positively charged Lys residue, bear the nitroxide-containing α-amino acid TOAC to study them using EPR spectroscopy. Vesicles were used to investigate orientation and penetration depth of the peptide at room temperature. Bicelles were employed to evaluate the order, dynamics, and orientation of the peptide at a near physiological temperature. In addition, the position of the N-terminal 1-octanoyl chain in the membrane was studied by labeling it with a nitroxide. The secondary structure of the peptides in vesicles was studied by CD spectroscopy showing that they adopt a mostly α-helical structure. In vesicles, the analogs insert below the lipid headgroups with the helix axis oriented parallel to the membrane surface at a peptide-to-lipid (*P*:*L*) ratio of 1:100. The presence of the single, positively charged Lys residue does not alter the orientation adopted by the peptides. In bicelles at *P*:*L* ratios 1:100 and 1:60, the peptide adopts a transmembrane orientation characterized by a very low orientational order, whereas at a 1:15 *P*:*L* ratio it severely disrupts the membrane. Our data shows that overall orientation and insertion in model membranes of the native trichogin GA IV are strictly comparable to those of its methyl ester analogs previously examined.

KEYWORDS
bicelles, circular dichroism, electron paramagnetic resonance, membranes, trichogin

1 | INTRODUCTION

Peptaibiotics are nonribosomally synthesized peptides that display a variety of biological effects, such as antibacterial, antiviral, or anticancer.[1] Their primary structures, composed by as few as 4 up to 20 residues, are characterized by (i) a high content of C^{α}-tetrasubstituted residues [in particular, α-aminoisobutyric acid (Aib, Scheme 1)], (ii) an acylated N-terminus, and (iii) a C-terminal 1,2-amino alcohol. All peptaibiotics are generally considered membranolytic agents, but while the 19-residue alamethicin, the most studied peptide of this family, forms voltage-dependent pores,[2] the detailed mechanism of action of shorter peptaibiotics is largely unknown.

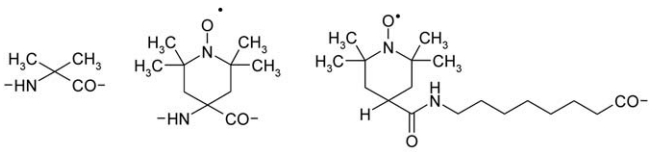

SCHEME 1 Chemical structures of Aib, TOAC, and TEMPO-CO-Aoc [1-oxyl-2,2,6,6,-tetramethylpiperidine-4-carb-(8-amido-1-octanoyl)]

Trichogin GA IV (TG) is a short peptaibiotic produced by the fungus *Trichoderma longibrachiatum*.[3–5] Its primary structure is Oct-Aib-Gly-Leu-Aib-Gly-Gly-Leu-Aib-Gly-Ile-Lol (Oct is 1-octanoyl, Lol is the 1,2-amino alcohol leucinol). To unravel the mechanism of action of TG and to possibly develop a drug from TG, in the last two decades we have been synthesizing selected TG analogs and investigating them by means of a variety of physicochemical techniques.[4–38] The presence of the three helix-inducing Aib residues allows TG to adopt a helical structure in the crystal state,[4] in organic solvents,[3,11,13,21] in membranes,[16] and in membrane mimetic environments.[5,15,20,21,23] Both its N- and C- terminal moieties play a crucial role in the antimicrobial and cytotoxic activity of this peptide.[24] In particular, we recently demonstrated the importance of its C-terminal Lol amino alcohol, as its replacement with a methyl ester (-Leu-OMe) or a carboxylic acid (-Leu-OH) determines a significant inhibition of the cytotoxic action.[24] This finding prompted us to revise some of the work previously performed on TG analogs not bearing an alcoholic function at the C-terminus.[6,7] In particular, we decided to verify by means of EPR if the presence of the native N- and C-terminal residues would have any effect on membrane orientation, penetration depth, and dynamics of the spin-labeled TG analogs.

Spin-labeling electron paramagnetic resonance (EPR) spectroscopy is a well-established technique for studying the interactions of peptides and proteins with lipid membranes, from liposomes to extracted cell membranes, providing a great amount of information on the solutes and on their molecular environment.[39] In particular, EPR can precisely determine the insertion depth of a solute relative to the plane of the phosphate groups of the bilayer.[40,41] This result can be achieved by comparing the data for the solute to those of a "molecular ruler", i.e., a series of phospholipids spin-labeled at different positions of their lipid tails.[41] EPR can also offer valuable insights on the orientation of the solutes in the membrane when the latter is macroscopically oriented.[42–44] Among model membranes, bicelles are the best for magnetic spectroscopies since they form oriented phases in the magnetic field of the spectrometer at physiological temperature and without the need of a solid support.[45,46] Since peptides are diamagnetic, a paramagnetic label must be introduced to use EPR spectroscopy. In the present work, we decided to exploit the nitroxide-containing α-amino acid 4-amino-1-oxyl-2,2,6,6-tetramethylpiperidine-4-carboxylic acid (TOAC, Scheme 1). As it belongs to the family of C^{α}-tetrasubstituted α-amino-acids, it can replace the strongly helicogenic Aib since it exhibits strictly comparable three-dimensional structural propensities.[47,48] In addition, the quite restricted mobility of the TOAC nitroxide side chain directly reflects that of the peptide backbone. For all these reasons, TOAC has been extensively used to correlate the biological and conformational properties of peptides.[49]

2 | EXPERIMENTAL

2.1 | Materials

Fmoc-TOAC-OH (Fmoc, fluorenyl-9-methyloxycarbonyl) was synthesized as previously reported.[47] H-L-Lol-2-chlorotrityl resin (200–400 mesh, loading 0.43 mmol/g resin) was purchased from Iris Biotech (Marktredwitz, Germany). Fmoc-amino acids were supplied by Novabiochem (Merck Biosciences, La Jolla, CA), and all other amino acid derivatives and reagents for peptide synthesis by Sigma-Aldrich (St. Louis, MO). 2-(1H-7-Aza-1,2,3-benzotriazol-1-yl)−1,1,3,3-tetramethyluronium hexafluorophosphate (HATU) was purchased from PE Biosystems (Warrington, UK). *N*-Ethyl, *N*′-[3-(dimethylamino)propyl]carbodiimide (EDC), 1-hydroxy-1,2,3-benzotriazole (HOBt), 7-aza-1-hydroxy-1,2,3-benzotriazole (HOAt), and 2-(1H-1,2,3-benzotriazol-1-yl)−1,1,3,3-tetramethyluronium hexafluorophosphate (HBTU) were Acros-Janssen (Geel, Belgium) products. 1,2-Dihexanoyl-*sn*-glycero-3-phosphocholine (DHPC), 1,2-dimyristoyl-*sn*-glycero-3-phosphocholine (DMPC), and 1-palmitoyl-2-oleoyl-*sn*-glycero-3-phosphocholine (POPC) were purchased from Avanti Polar Lipids (Alabaster, AL) as chloroform solutions. Methanol, 99.9%, spectrophotometric grade, and [4-(2-hydroxyethyl)−1-piperazinyl]ethanesulfonic acid (HEPES) and the lanthanide salts $TmCl_3{\cdot}6H_2O$ and $DyCl_3{\cdot}6H_2O$ were obtained from Sigma-Aldrich. A 50 mM, pH 7.0, HEPES buffer solution was prepared to be used for liposomes and bicelle preparations, and for the stock solutions of the Tm^{3+} and Dy^{3+} salts as well.

2.2 | Peptide synthesis

TG was synthesized as previously published,[20] while the synthetic procedure for [$TOAC^1$] TG and [$TOAC^1$, Lys^6] TG has been recently reported.[50] In this work, we synthesized five new analogs of TG (Table 1). All peptides were prepared by manual solid-phase peptide synthesis (SPPS), exploiting a previously described synthetic strategy.[20,21] The reactivity of TOAC in peptide bond formation is similar

TABLE 1 Name, Primary Structure, Net Charge, Mean Residue Hydrophobicity (H), Mean Hydrophobic Moment (μ), and CD R Value in SUV for the Peptides Studied in This Work.

Peptide	Primary structure[a]	Net charge	H	μ	$R^{SUV} = [\theta]_{222}/[\theta]_{208}$
TG	*Oct*-UGLUGGLUGI-Lol	0	5.2	3.09	0.70
[TOAC^1] TG	*Oct*-**X**GLUGGLUGI-Lol	0	5.2	3.08	0.63
[TOAC^1, Lys^6] TG	*Oct*-**X**GLUG**K**LUGI-Lol	+1	4.5	3.61	0.58
[TOAC^4] TG	*Oct*-UGL**X**GGLUGI-Lol	0	5.2	3.07	0.61
[TOAC^4, Lys^6] TG	*Oct*-UGL**X**G**K**LUGI-Lol	+1	4.5	3.60	0.61
[TOAC^8] TG	*Oct*-UGLUGGL**X**GI-Lol	0	5.2	3.08	0.65
[Lys^6, TOAC^8] TG	*Oct*-UGLUG**K**L**X**GI-Lol	+1	4.5	3.61	0.65
[TEMPO^0] TG	*TEMPO-CO-Aoc*-UGLUGGLUGI-Lol	0	5.0	3.06	0.50

[a]U, Aib; **X**, TOAC.

to that of Aib.[47,48] Thus, the same coupling procedure was employed for both residues. The whole synthetic protocol is very fast (less than 24 h per batch). Moreover, the excess reagents employed per coupling step were low (1 equivalent excess), even when Aib or TOAC residues were involved.

[TEMPO^0] TG was synthesized similarly to TG up to the deprotection step of the N-terminal Aib residue.[20] Then, Fmoc-Aoc-OH was inserted using HATU and *N*,*N*′-diisopropylethylamine as coupling reagents. After Fmoc deprotection and acylation with 4-carboxy-TEMPO (Sigma Aldrich), mediated by EDC and HOAt, the desired peptide was obtained.

For both [TOAC^4, Lys^6] TG and [Lys^6, TOAC^8] TG analogs, an acidic treatment was required, in the presence of the nitroxide, for Boc removal. To this end, the peptides were left for 2 h in a solution of 3M HCl in methanol (MeOH). This procedure involves a reversible loss of the radical moiety, as highlighted by HPLC analysis. The nitroxide integrity was completely recovered by treatment with an aqueous solution of NH_4OH 1M for about 6 h.

The purities of the crude peptides were all above 90%. All peptides were purified either by medium-pressure liquid chromatography (Isolera Prime system, Biotage, Sweden) or by preparative HPLC on a Phenomenex C_{18} column (30 × 250 mm, particle size: 5 μm), using a Shimadzu (Kyoto, Japan) LC-8A pump system (flow rate 15 mL/min) equipped with a SPD-6A UV-detector ($\lambda = 216$ nm) and a binary elution system: A, H_2O + 0.05%TFA(trifluoroacetic acid); B, CH_3CN/H_2O (9:1 v/v) + 0.05%TFA to reach a final purity >96%. The yields after purification were within the range 60% to 80%. The purified fractions were characterized by analytical RP-HPLC on a Jupiter Phenomenex (Torrance, CA) C_{18} column (4.6 × 250 mm, 5 μm) using an Agilent (Santa Clara, CA) 1200 HPLC pump. The binary elution system used was: A, H_2O/CH_3CN (9:1 v/v) + 0.05%TFA; B, CH_3CN/H_2O (9:1 v/v) + 0.05%TFA; gradient 60% to 90% B in 20 min (flow rate 1 mL/min); spectrophotometric detection at $\lambda = 216$ nm. Electrospray ionization mass spectrometry (ESI-MS) was performed by using a PerSeptive Biosystem Mariner instrument (Framingham, MA). The new TG analogs were characterized by ESI-MS and HPLC analysis as follows:

[TOAC^4] TG ESI-MS *m/z*: calculated for $C_{58}H_{105}N_{12}O_{13}$ 1177.79, found 1177.78

t_R = 13.3 min (gradient: 70%–100%B in 20 min)

[TOAC^4, Lys^6] TG ESI-MS TGESI-MS *m/z*: calculated for $C_{62}H_{114}N_{13}O_{13}$ 1248.87, found 1248.84

t_R = 18.7 min (gradient: 50%–80%B in 20 min)

[TOAC^8] TG ESI-MS *m/z*: calculated for $C_{58}H_{105}N_{12}O_{13}$ 1177.79, found 1177.785

t_R = 14.7 min (gradient: 70%–100%B in 20 min)

[Lys^6, TOAC^8] TG ESI-MS *m/z*: calculated for $C_{62}H_{114}N_{13}O_{13}$ 1248.87, found 1248.83

t_R = 24.1 min (gradient: 30%–100%B in 30 min)

[TEMPO^0] TG ESI-MS *m/z*: calculated for $C_{62}H_{112}N_{13}O_{14}$ 1262.85, found 1262.88

t_R = 14.9 min (gradient: 45%–60%B in 20 min)

2.3 | CD spectroscopy in liposomes

The small unilamellar vesicles (SUV) used in this study were prepared from POPC. The lipids were dissolved in chloroform and a homogeneous lipid film was obtained by drying the solution under a gentle stream of dry nitrogen. The film was left overnight under vacuum in a desiccator to remove any trace of solvent. The following day a dilute HEPES buffer (5 mM) was added to the film to obtain a 10 mM lipid concentration. SUV in the 30 to 50 nm diameter range were prepared by sonication: the lipid suspension was immersed in a water bath and sonicated until the solution started to clear. SUV dimensions were checked during preparation by

dynamic light scattering using a NICOMP Model 370 submicron particle sizer. Vesicles were used immediately after preparation.

The peptide was incorporated into the liposomes by adding a small amount of a MeOH stock solution into an Eppendorf tube. The concentration of the peptide stock solutions was about 1 mM. MeOH was then evaporated under a gentle stream of nitrogen and the residue dissolved in a small amount of buffer and sonicated for 3 min. Lastly, a proper amount of POPC SUV solution was added to obtain a final POPC concentration of 2 mM and a final peptide concentration of 0.1 mM. CD spectra were recorded at 293 K using a Jasco (Tokyo, Japan) model J-715 spectropolarimeter, equipped with a Haake thermostat (Thermo Fisher Scientific, Waltham, MA), averaging 36 scans. Baselines were corrected by subtracting the liposome contribution. A cylindrical, fused quartz cell of 0.1 mm path length (Hellma, Müllheim, Germany) was employed. The data are expressed in terms of $[\theta]_T$, the total molar ellipticity (deg.cm^2.dmol^{-1}).

2.4 | EPR experiments in liposomes

EPR spectra and power saturation experiments were recorded in POPC liposomes prepared in the same way as those used for CD experiments. The values of the immersion depth for the spin labeled lipids have been recently published by some of us.[51] Peptides were incorporated in to the liposomes as follows: a MeOH solution of the peptide was evaporated in an Eppendorf tube. The preformed liposomes were added. The solution was then sonicated for 3 min. EPR experiments were performed using a Bruker ESP380 spectrometer operating at X-band (~9.5 GHz), equipped with a room-temperature dielectric resonator, ER4123D. The microwave frequency was measured by a frequency counter, HP5342A. All spectra were obtained using the following parameters: modulation amplitude 0.16 mT; modulation frequency 100 kHz; time constant 41 ms; conversion time 82 ms; scan width 1.25 mT; 512 points; temperature 298 K. The microwave power for saturation experiments was ramped down automatically from 95 mW to 0.05 mW (the attenuation ramp in dB units was 2.0, 4.0, 6.0, 8.0, 10.0, 12.0, 14.0, 16.0, 18.0, 20.0, 25.0, 30.0, 35.0). The spectra at each power were averaged three times. The experimental protocol for the insertion depth measurements is as follows: approximately 5 μL of sample were loaded into a gas-permeable TPX capillary (L&M EPR Supplies, Milwaukee, WI) and three saturation experiments were performed. The first experiment was carried out on the sample in equilibrium with air to saturate the membrane with oxygen. The second experiment was performed on the same sample after deoxygenation under a dry nitrogen flow for 20 min. The third experiment was carried out on a new sample to which Ni(II) ethylendiamino-*N*,*N*'-diacetate (NiEDDA) was added to a final concentration of 50 mM (the sample was then deoxygenated as above). All experiments were performed at least in duplicate. The power saturation data were obtained using a home-written program in Matlab that calculates the peak-to-peak amplitudes of the central line of the spectra. The saturation curves were obtained by plotting the amplitude data *vs* the microwave power, and fitted using the standard equation:[9] $y = A \cdot p_{1/2} \cdot [1 + (2^{1/h} - 1) \cdot x/p_{1/2}]^{-h}$ where $p_{1/2}$ is the saturation parameter, namely the power where the first derivative amplitude is reduced to half of its unsaturated value, h is the homogeneity parameter, indicating the homogeneity of saturation of the resonance line (ranging between $h = 1.5$ for a fully homogeneous line and $h = 0.5$ for a fully inhomogeneous line), and A is a scaling factor that accounts for the absolute signal intensity. The dimensionless immersion depth parameter (Φ) can be directly calculated from the ratio of the $p_{1/2}$ parameters obtained from the fitting of the three experiments described above: $\Phi = \ln \frac{p_{1/2}^{\text{oxygen}} - p_{1/2}^{\text{nitrogen}}}{p_{1/2}^{\text{NiEDDA}} - p_{1/2}^{\text{nitrogen}}}$.

The Φ parameter can be used to assess the distance from the membrane surface (R) of a solute, provided a calibration curve is calculated.[52,53] Previously, we calculated the calibration curve from all spin labeled lipids (SL).[54] Here, we recalculated the curve by removing the 5DPC (1-palmitoyl-2-stearoyl-*sn*-glycero-5-doxyl-3-phosphocholine) label from the linear regression, since its depth parameter is not linearly correlated to the distance from the membrane surface. The new equation is R (/nm) = 0.34(±0.03)· Φ + 0.70(±0.05).

2.5 | EPR experiments in bicelles

The chloroform solutions of the phospholipids and a MeOH solution of [TOAC^4, Lys^6] TG were mixed in a glass test tube. Samples at different peptide concentrations were prepared by keeping the lipid content constant and varying the amount of peptide to obtain the desired *P*:*L* ratio (the *P*:*L* ratios reported in this work refer to DMPC only). The final lipid composition of the solution was: 11.2 μmol DMPC, 3.1 μmol DHPC; the q = [DMPC]/[DHPC] ratio was therefore ~3.5. A thick film, containing the lipids and the peptide, was produced by evaporation of the solvent under a stream of dry nitrogen gas, then the film was dried under vacuum overnight. The following day the film was scratched off the glass tube and placed into an Eppendorf tube. Then, 33 μL of buffer were added, obtaining a 25% (w/w) lipid concentration. The resulting suspension was vortexed until it appeared homogeneous. The sample was then placed in a bath sonicator that was filled with an ice/water mixture and sonicated for 30 min. Finally, the solution was subjected to four freeze/thaw cycles: 30 min in a 328 K water bath were followed by a quick freeze in liquid nitrogen; vortexing of the sample at each step was performed to insure perfect homogeneity. The procedure yielded a clear, viscous, stock of bicelles with the peptide incorporated in the bilayers. The EPR samples were prepared as

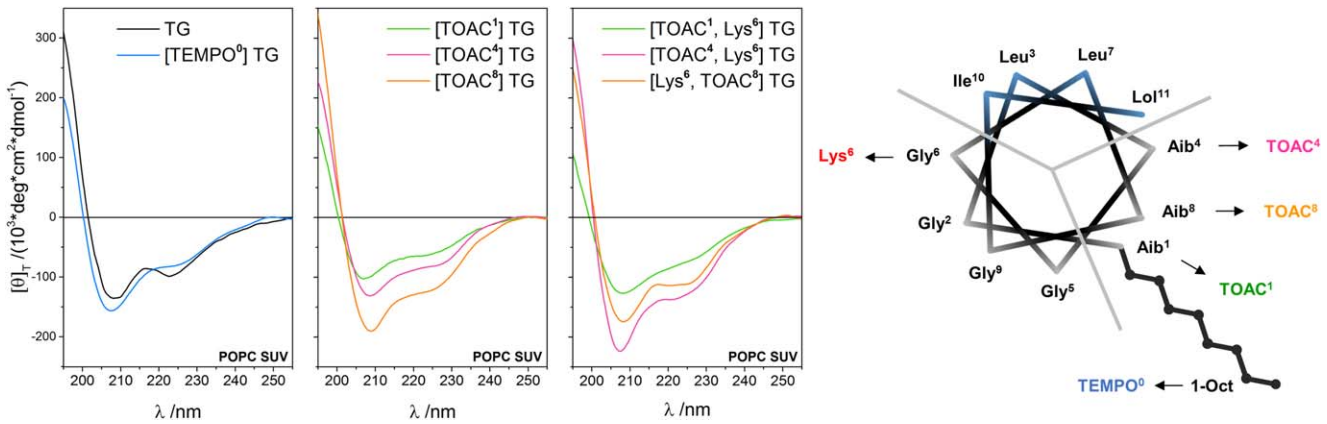

FIGURE 1 Left: CD spectra in SUV solutions of the analogs discussed in this work. Right: Helical wheel representation of trichogin GA IV divided into three sectors. The arrows indicate positions and nature of the substitutions characterizing the newly synthesized analogs

follows: 15 μL of bicelle stock were added to 10 μL of buffered solution of Tm^{3+} or Dy^{3+} (corresponding to a final [Ln^{3+}]/[DHPC] ratio of 0.9). The resulting solution was transferred to a 1-mm inner diameter EPR quartz tube. The final concentration of the phospholipids was 17% (w/w). Given the experimental conditions (lipid concentration, *q* ratio, temperature), the bicelles used in this work are not ideal disks, but rather stacks of almost planar phospholipid bilayers dotted with DHPC pores and separated by buffer regions ~15 nm wide.[55] A literature procedure[45] was used to obtain aligned samples: the sample tube was placed at room temperature (~298 K) in the EPR cavity and the magnetic field was set to 800 mT. Then, the temperature was slowly raised to 318 K and subsequently lowered to the temperature of choice, 308 K. The magnetic field was set to ~350 mT and the spectrum was recorded immediately after. Loss of order in the sample during the measurement time (~40 s) is negligible as a result of the high viscosity of the bicelle solution which prevents lipid reorientation. For each sample, the experiments were repeated with Tm^{3+} or Dy^{3+} as dopants, to align the membrane normal parallel or perpendicular to the external magnetic field. EPR spectra of the peptide in bicelles were recorded using a Bruker ER200D spectrometer operating at X-band (~9.5 GHz), equipped with a rectangular cavity (ER4102ST) fitted with a cryostat, and a variable-temperature controller (Bruker ER4111VT). The microwave frequency was measured by use of a frequency counter (HP5342A). All spectra were obtained in a single scan using the following parameters: microwave power 2.1 mW; modulation amplitude 0.16 mT; modulation frequency 100 kHz; time constant 20 ms; conversion time 41 ms; scan width 15 mT; 1024 points; temperature 308 K.

2.6 | EPR spectra simulations

The spectra of the TG analogs in SUV and bicelles were simulated with a program based on the stochastic Liouville equation,[56] that is extensively used for nitroxides.[57–64] The simulation method relies on several reference systems, the relative orientation of which is defined by different sets of Euler angles.[56] The orientations of the principal diffusion axes relative to the *g* tensor reference frame (Ω_D) were estimated from the crystal structures of TOAC-labeled TG analogs.[13] The starting values for the principal components of the *g* and ^{14}N hyperfine (*A*) tensors of the TOAC label were obtained from the literature.[59,65] The final values of the *g* and *A* tensors, the main values of the diffusion tensor (*D*), the order parameter of the peptide (*S*), and the orientation of the magnetic field relative to the average long diffusion axis (Ψ) were obtained from the simulations that were optimized by simplex fitting. Note that in the fitting of the spectra there might be some correlation between the hyperfine values mediated by the molecular motion and the calculated diffusion tensor. However, the hyperfine values obtained for the three TOAC-containing TG analogs are corroborated by the results from the membrane penetration depth experiments (see below).

3 | RESULTS AND DISCUSSION

3.1 | Peptide secondary structure in the membrane

The secondary structures of TG and its analogs were studied by means of electronic CD spectroscopy in POPC SUV at a peptide/lipid ratio of 1:20 to assess their secondary structure in bilayer membranes (Figure 1, left). For all analogs, we observed two negative Cotton effects at 204 to 210 nm and 220 to 224 nm and a positive Cotton effect just below 195 nm. These features are typical of right-handed helical conformations. The first two negative maxima are related to the parallel component of the $\pi \rightarrow \pi^*$ transition and the $n \rightarrow \pi^*$ transition of the peptide chromophore, respectively,

while the positive maximum is related to the perpendicular component of the $\pi \rightarrow \pi^*$ transition.[66,67]

An estimation of the helical type (whether 3_{10}- or α-) can be achieved by measuring the ratio of the two negative ellipticity maxima,[66–69] $R = [\theta]_{222}/[\theta]_{208}$ (Table 1). The R^{SUV} value for TG and its analogs in POPC ranges from 0.50 to 0.70. These values are consistent with the presence of a predominantly α-helical conformation. Therefore, we plotted TG according to an α-helical wheel representation (Figure 1, right) to evaluate the spatial distribution of the residues. We observed a mildly hydrophilic sector (about 140° wide) consisting only of Gly residues, a highly hydrophobic sector (120° wide) composed of Leu/Ile/Lol, and a "structural" sector (roughly 100° wide) where the three helix-promoting Aib (or TOAC) residues are located.

3.2 | Peptide hydrophobicity and hydrophobic moment

We calculated the mean hydrophobicity per residue (H) and mean hydrophobic moment (μ) for all TG analogs (Table 1). These two parameters are widely used to characterize peptide sequences.[70] The H parameter depends only on the primary structure and is higher for more hydrophobic peptides, while μ is a vector that represents the amphipathicity of the peptide and therefore depends on its secondary structure. In the calculations we used a modified version of the Combined Consensus Hydrophobicity Scale (CCS) developed by Tossi et al.[71,72] The CCS scale was chosen since it quantifies the hydrophobicity of some non-coded amino acids, including Aib. We extended the CCS scale to the values for TOAC, Lol, and Oct, as previously described,[50] and that for TEMPO-CO-Aoc moiety.

Given the information extracted from the CD spectra (Figure 1), in the calculation of the hydrophobic moment for TG we assumed a fully α-helical structure. In the crystal state, the 3_{10}-helical portion is confined to the three N-terminal residues.[4] A different conformation for the first three residues does not significantly influence either the H or the μ parameter. The analogs with Lys at position 6 are more hydrophilic (Table 1), as expected. Since position 6 falls in the hydrophilic face of the peptide, the introduction of a more polar amino acid (Lys^6 vs Gly^6) increases markedly its overall amphipathicity.

3.3 | Peptide motion in SUV

The EPR spectra of the TG analogs in POPC SUV, recorded at room temperature (298 K) and at low microwave power (2 mW), are reported in Figure 2. The lineshape of the EPR spectrum of a TOAC-labeled peptide is determined by its motion, which, in turn, is influenced by the peptide secondary structure and its partition into the membrane. Peptides that are unfolded and not bound to a membrane show spectra

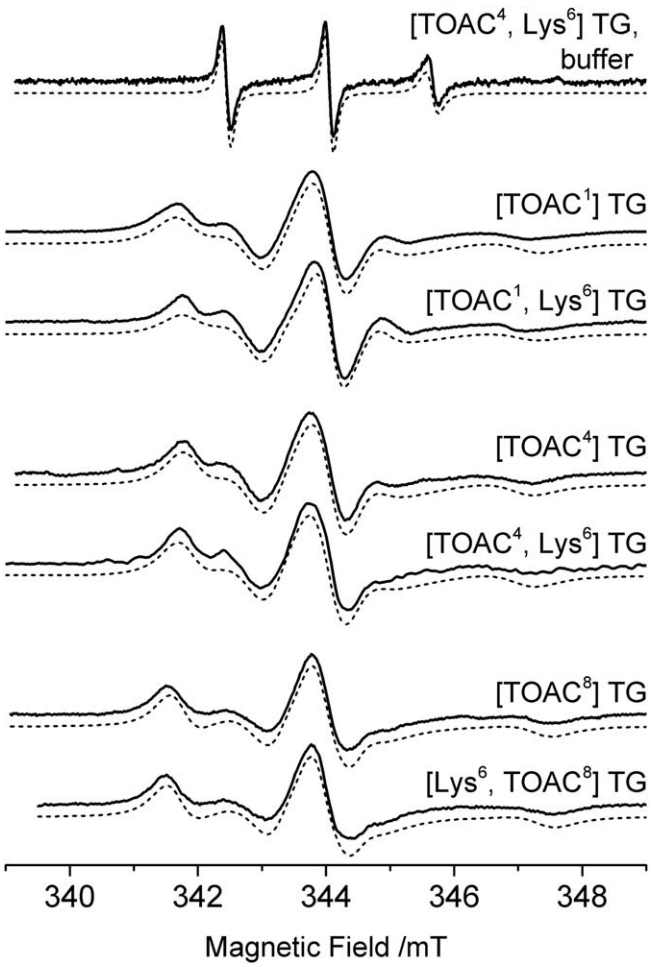

FIGURE 2 Experimental EPR spectra (solid lines) and simulations (dashed lines) for the TOAC-labeled peptides. On top, the room temperature spectrum of [$TOAC^4$, Lys^6] TG in buffer (all other spectra are in POPC SUV)

that are in the fast motion regime (three narrow EPR lines), while peptides that are folded into an helical secondary structure or bound to the membrane are characterized by spectra that are in the slow motion regime (a wide lineshape with broad lines). The dynamics of the peptide are expressed in terms of the rotational diffusion tensor D or the correlation time τ (see below). The EPR spectra of a nitroxide also reports on the polarity of the environment through the ^{14}N hyperfine coupling, in particular the A_{zz} principal component of the A tensor. A nitroxide dissolved in increasingly polar environments shows progressively broader EPR spectra. Information on dynamics and polarity that are qualitatively evaluated from the spectral lineshape can be quantitatively analyzed by performing simulations with models of various complexity.

The Microscopic Order Macroscopic Disorder (MOMD) model,[56] or the even more complex Slowly Relaxing Local Structure (SRLS),[73] is commonly used for the simulations of the EPR spectra of labeled proteins and peptides in SUV.

TABLE 2 Parameters Obtained from the Fitting of the EPR Spectra in POPC SUV.

	Hyperfine tensor (mT)			Diffusion tensor (MHz)			Correlation time (ns)
Peptide	A_{xx}	A_{yy}	A_{zz}	D_{iso}	$D_{\|\|}$	$D_{\perp}$	τ
[TOAC^{1}] TG	0.65	0.65	3.25	17	-	-	10
[TOAC^{1}, Lys^{6}] TG	0.65	0.65	3.27	21	-	-	8
[TOAC^{4}] TG	0.64	0.66	3.07	14	-	-	12
[TOAC^{4}, Lys^{6}] TG	0.61	0.62	3.11	13	-	-	13
[TOAC^{8}] TG	0.75	0.50	3.23	-	61	9	18
[Lys^{6}, TOAC^{8}] TG	0.75	0.50	3.25	-	86	8	21

The g tensors for all peptides are $g_{xx} = 2.0096$; $g_{yy} = 2.0064$; $g_{zz} = 2.0035$.

Nevertheless, we chose a simpler simulation model for TG. In our model, the labeled peptide experiences an isotropic or axial motion, the magnetic and diffusion axes are considered co-linear, and no effects of local ordering are contemplated. Our choice was guided by the experiments in bicelles (see below) that demonstrated that the microscopic order displayed by TG is extremely low, thereby reducing the need for the more complex models. The simulations allowed us to gain information on the rotational dynamics of the peptides, obtained as the diffusion tensor D. The dynamics are more

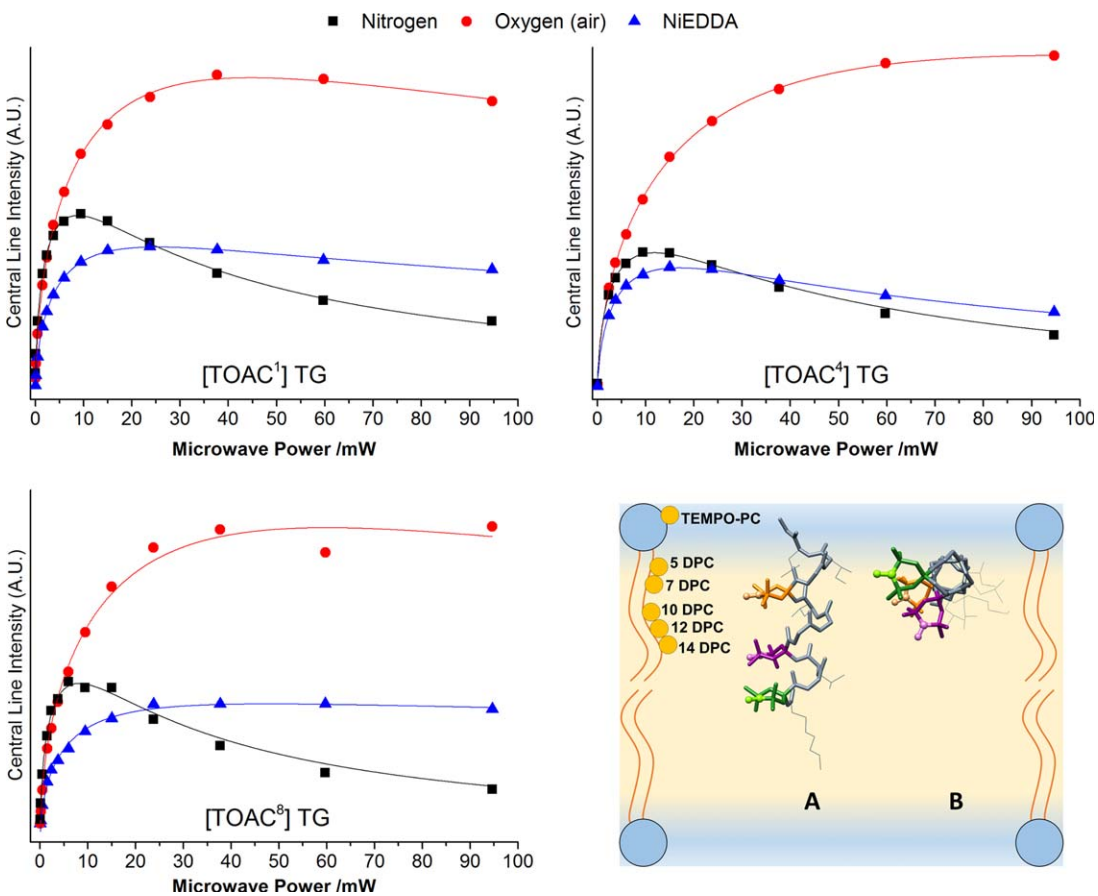

FIGURE 3 Penetration depths of the three TOAC-labeled TG analogs in POPC SUV (power saturation data with the corresponding fitting curves as full lines). Each symbol indicates a different experimental condition: black squares, sample purged with nitrogen; red dots, sample in equilibrium with air (oxygen); blue triangles, sample with 50 mM NiEDDA and purged with nitrogen. The experiments were performed at room temperature at *P*:*L* 1:100. The cartoon shows the in-scale POPC membrane and positions of the lipid spin labels (yellow dots) as well as two possible orientations for the TG helix in SUV: (A) transmembrane, (B) parallel to the membrane surface

TABLE 3 Penetration Depth Parameter (Φ) for the Reference Spin Labeled Lipids (SL) and the TG Analogs Studied in This Work in POPC Liposomes Obtained at Room Temperature.

SL	Φ (±0.1)	Peptide	Φ (±0.1)	R (nm) (±0.1)
TempoPC	−0.1[a]	[TOAC^1] TG	0.9	1.0
5DPC	1.4[b]	[TOAC^1, Lys^6] TG	1.0	1.0
7DPC	1.2[b]	[TOAC^4] TG	2.9	1.7
10DPC	2.1	[TOAC^4, Lys^6] TG	2.7	1.6
12DPC	2.4	[TOAC^8] TG	1.4	1.2
14DPC	3.0	[Lys^6, TOAC^8] TG	1.8	1.3

Absolute depth R (nm) of the two peptides calculated as described in the Experimental section. The Φ values have been obtained as the average of the results of at least two experiments.
[a]Repeated experiments with TempoPC showed a large variability in Φ, but the value is always <0.3.
[b]An inversion in the linear trend was found also in the original work.[41]

conveniently discussed in terms of the rotational correlation time τ.[74] For an isotropic rotational motion $\tau = 1/(6 \cdot D_{iso})$, where D_{iso} is the isotropic diffusion tensor. For an axial rotation, the diffusion tensor is characterized by two main values, $D_{||}$ and $D_{\perp}$, and, when $D_{||} > D_{\perp}$, $\tau \approx 1/(6 \cdot D_{\perp})$.[74] We also refined the literature principal values of the ^{14}N hyperfine coupling tensor A by fitting. The relevant parameters derived from the spectra simulations are reported in Table 2.

As an example, on top of Figure 2 we report the EPR spectrum of [TOAC^4, Lys^6] TG in buffer solution. The spectrum exhibits the three sharp lines typical of TG analogs in buffer, where the peptide backbone is at least partially unfolded.[50] This pattern originates from the fast motion of the TOAC nitroxide that reflects the closely related one of the peptide backbone. From the fitting, we obtain the isotropic hyperfine coupling $A_{iso} = 16.1$ mT and a correlation time $\tau = 0.5$ ns. All other peptides in buffer have nearly identical lineshapes (data not shown).

The spectra of the peptides in POPC SUV have much broader lineshapes than those of the peptides in buffer solution. These patterns are indicative of the slowdown of the nitroxide motion caused by its incorporation in the liposomes. Given the absence of sharp lines in the spectra, the incorporation is quantitative.

The spectra show that the Gly-to-Lys substitution at position 6 has little influence on the peptide conformation and position in the membrane, since no significant differences in dynamics or hyperfine parameters are obtained from the fitting. On the contrary, the spectra of the TOAC-labeled analogs (at position 1, 4, or 8) are similar, but not identical, thus suggesting that the three positions of the helix where TOAC is inserted have slightly different environments and/or dynamics. Indeed, from the fitting of the experimental spectra, we observed that the A_{zz} hyperfine values (the parameter most sensitive to the polarity of the environment) are very close for the peptides bearing TOAC at position 1 or 8, and significantly lower for those with TOAC at position 4. Since a low value of the A_{zz} component corresponds to an apolar environment, the simulations suggest that the TOAC nitroxides at position 4 are buried deeper in the membrane than those at the other two positions. This observation is discussed in more detail below (see Penetration depth and orientation in SUV). The dynamics of the peptides are more varied. TOAC positions 1 and 4 display a remarkable isotropic motion, while position 8 can be simulated only by introducing an axial motion. In particular, the diffusion is faster around the main axis and slower along the axes perpendicular to it ($D_{||} > D_{\perp}$). All TOAC positions show very similar correlation times τ, but with TOAC at position 8 an overall slower dynamics is observed.

3.4 | Penetration depth and orientation in SUV

The penetration depth of the TG analogs in POPC SUV at P:L 1:100 at room temperature were determined by power saturation experiments.[41] These measurements allow one to obtain the exact position of the nitroxide moiety in a lipid bilayer. Additionally, the combined knowledge of the penetration depth of the TOAC-labeled analogs permits one to model the orientation of the peptide in the membrane. In Figure 3, the results of the power saturation experiments for the TG analogs labeled with TOAC at position 1, 4, or 8 are reported. The fitting curves were obtained according to the equation reported in the Experimental section. The penetration depth parameters Φ for all peptides are listed in Table 3 along with those previously determined for the spin-labeled lipids, acting as "molecular ruler",[41,51] and the distance from the membrane surface (R),[52] calculated as reported in the Experimental section.

For all peptides, the penetration depths of the labels at different positions increase in the rank order TOAC^1 < TOAC^8 < TOAC^4. TOAC^1 is positioned above

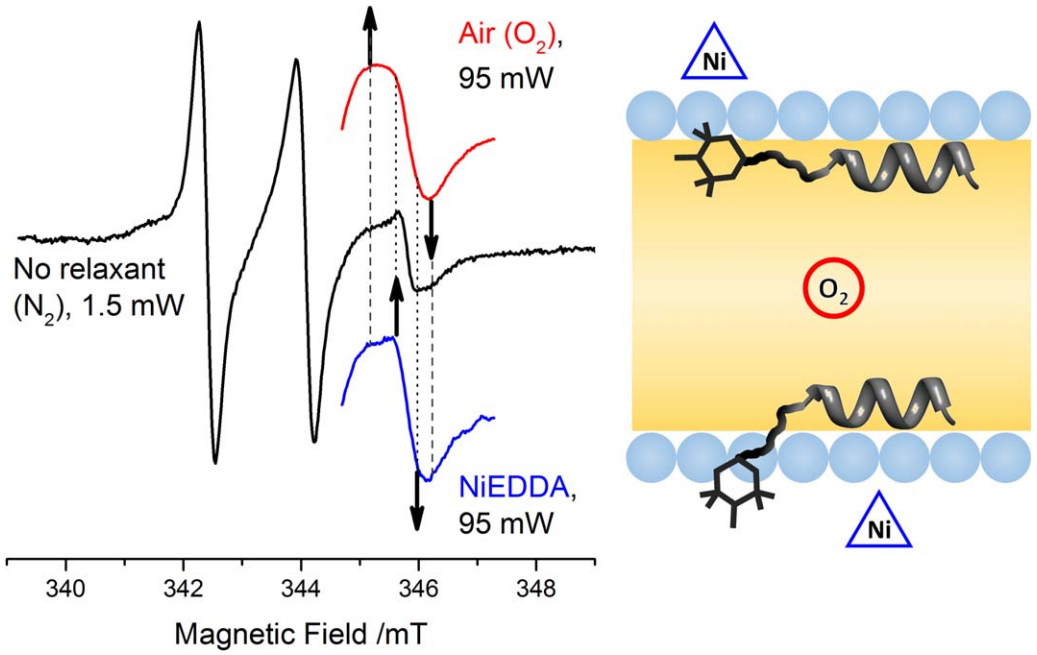

FIGURE 4 Left, in black, EPR spectrum of the [TEMPO^0] TG at low power in POPC SUV, *P*:*L* 1:100, room temperature; in colored lines, the high field line at high power in the presence of oxygen (red, top), and in the presence of 50 mM NiEDDA (blue, bottom). Right, cartoon of [TEMPO^0] TG showing the possible positions of the TEMPO-CO-Aoc- moiety based on the EPR data

the fifth carbon atom of the lipid chains, TOAC^8 locates between the 5th and the 10th carbon atoms, and TOAC^4 is below the 12th carbon. To clarify the topology of the peptide in the membrane, we calculated the distances from the membrane surface (*R*) of the peptides and then compared them with the experimental bilayer thickness of POPC (3.91 nm at 30°C).[75] We modeled the peptides starting from the crystal structure of a TG analog[6] and adding the third TOAC label to the structure. The in-scale cartoon of the transmembrane (*A*) and parallel (*B*) orientations of the TG helix in the POPC membrane is illustrated in Figure 3. In the parallel orientation, the mildly hydrophilic sector of the TG helix (Figure 1) points towards the polar lipid headgroups, while the hydrophobic sector is facing the membrane interior. In this orientation, TOAC^1 and TOAC^8 (green and orange in Figure 3) have approximately the same penetration depth, while TOAC^4 (purple) points deeper towards the membrane interior. On the other hand, in any transmembrane orientation TOAC^1 and TOAC^8 show very different depths, both when the N-terminus is buried in the lipid bilayer (Figure 3) and when the N-terminus faces the headgroups (not reported). Therefore, the trend of the penetration depths clearly points to an orientation of the helix parallel to the bilayer surface for both TOAC^1 and TOAC^8 TG analogs, with or without Lys, in POPC SUV at a *P*:*L* 1:100. A parallel orientation for TOAC-labeled TG analogs was also obtained in other EPR studies. TG analogs where the C-terminal 1,2-amino alcohol (Lol) is replaced by a -Leu^{11}-OMe residue, were studied in egg-PC LUV at 300 K and *P*:*L* 1:260.[7] It was found that their TOAC^1, TOAC^4, and TOAC^8 residues are located, respectively, about 0.60, 0.75, and 0.70 nm from the phosphate groups, which correspond to an absolute depth (*R*) of about 1.10, 1.25, and 1.20 nm. Moreover, TG analogs where the N-terminal Oct chain is substituted by a Fmoc group and the C-terminal Lol by the -Leu^{11}-OMe residue were investigated in frozen DPPC at *P*:*L* 1:250 by electron spin echo envelope modulation (ESEEM) experiments.[18] In these cases, both TOAC^1 and TOAC^8 residues lie above the 9th-11th carbon atom of the lipid chain (i.e., $R < 1.40$ nm), whereas the TOAC^4 residue is located below its eleventh carbon atom (i.e., $R > 1.50$ nm).

It is worth noting that a change in orientation at higher *P*:*L* ratio cannot be ruled out. Indeed, in a slightly longer (14-amino acid long) peptaibiotic, ampullosporin A, we observed a switch from parallel to transmembrane orientation in POPC SUV on going from *P*:*L* 1:100 to 1:25.[54]

3.5 | Position of the octanoyl chain

The [TEMPO^0] TG analog was synthesized to study the position of the Oct chain in the bilayer. The EPR spectrum of this analog in SUV recorded under nonsaturating conditions is reported in Figure 4. The motion of the TEMPO-CO-Aoc- chain, and thereby the related EPR spectrum, is likely to be influenced by the peptide partition into the membrane. The spectrum of [TEMPO^0] TG is the sum of two components neither of which is in the fast motion regime, thus suggesting that both components arise from the TEMPO-CO-

Aoc- chain attached to a peptide immersed in the POPC membrane.

A complete overlapping of the two components impairs the immersion depth analysis. In principle, we could perform the analysis of the relaxation curves as the sum of two independent components, each characterized by a different $p_{1/2}$ value. However, the fitting of the central line fails to return two independent values for the $p_{1/2}$ parameters. Thereby, we performed the fitting with a single component that reflects the average penetration depth of the TEMPO moiety. The analysis shows a high water exposure of the TEMPO label ($\Phi = 0.0$).

The spectra of the peptide can be qualitatively analyzed to obtain some additional insight on the individual penetration depth of the two components. In Figure 4, we also report the high field line at high power in the presence of oxygen (top) or NiEDDA (bottom). Relative to the spectrum in non-saturating conditions, the spectrum with oxygen shows a preferential desaturation of the broader component, which results in a higher intensity of the outer edges of the line relative to the inner maxima. On the contrary, the spectrum with NiEDDA shows a greater desaturation of the narrower component. The trends in the intensities are highlighted by the arrows in the Figure 4. Therefore, assuming that the TG helix adopts a parallel orientation as discussed above, we suggest for the TEMPO-CO-Aoc- moiety the orientation sketched in the cartoon on the right side of Figure 4: the broader component belongs to a TEMPO label that is located inside the bilayer in a polar region, likely just below the polar headgroups (top), while the narrower component comes from a TEMPO label that points further out of the bilayer towards the aqueous phase (bottom).

Our data demonstrate that the TEMPO-CO-Aoc- moiety is either located parallel to the membrane surface or points towards the aqueous phase. The first orientation is not in contrast with the current hypothesis that the Oct chain acts as a hydrophobic anchor for TG,[4,13] while the second one is rather surprising. However, since the TEMPO label is known to have good affinity for the aqueous phase, it is quite reasonable that the Oct chain would be "dragged" towards it by the label. Thereby, it is highly unlikely that the water exposed orientation would be a genuine, intrinsic orientation of the unlabeled chain.

3.6 | Peptide order and orientation in bicelles

To achieve further insights into the membrane behavior of TG, we also investigated its order and orientation in magnetically-aligned DMPC/DHPC bicelles. We decided to perform the experiments with the [TOAC^4, Lys^6] TG analog since position 4 was shown to be particularly important for the proper folding of the peptide.[19–21] The Aib-to-Leu substitution results in a peculiarly bent crystalline structure,[21]

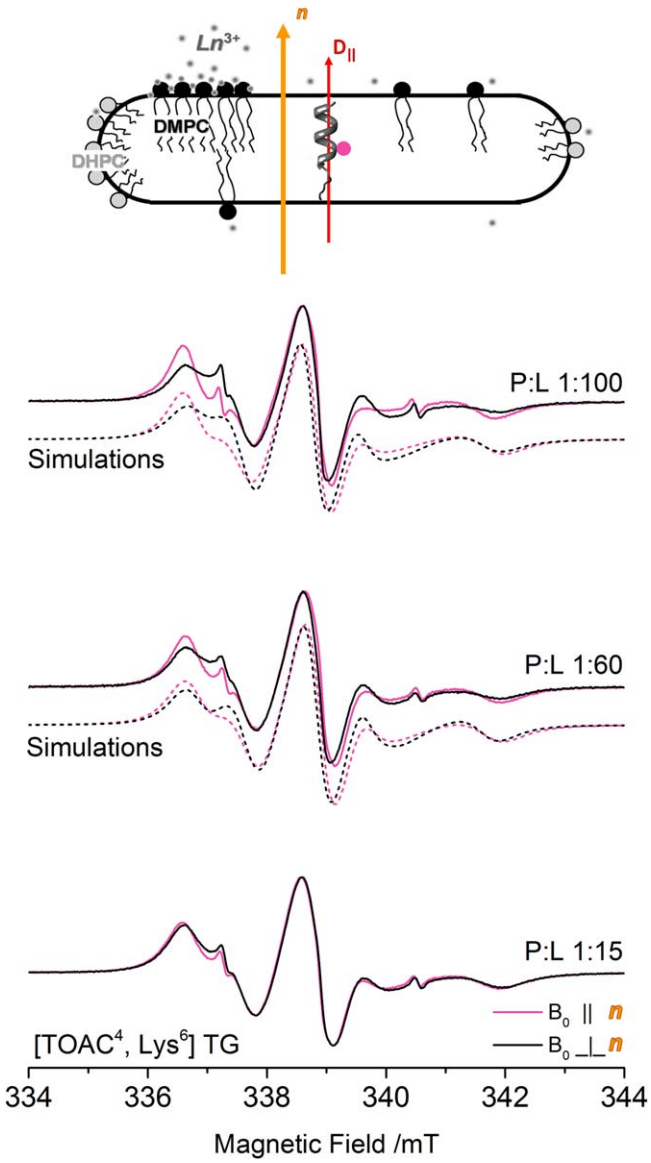

FIGURE 5 Top, schematic representation of a bicelle. The cartoon shows the long chain phospholipids (DMPC), the short-chain phospholipids (DHPC), and the lanthanide ions (Ln^{3+}, either Tm^{3+} or Dy^{3+}) used to align the membrane normal (n) either parallel or perpendicular to an external magnetic field. The cartoon also shows the TG helix in a transmembrane orientation, with the main diffusion axis ($D_{||}$) parallel to the membrane normal. For the abbreviations, see Experimental section. Bottom, EPR spectra (solid lines) and simulations (dashed lines) of [TOAC^4, Lys$^{[6]}$] TG in DMPC/DHPC bicelles at 308 K. The spectra have been recorded at *P*:*L* 1:100 (top), 1:60 (middle), and 1:15 (bottom) ratios and all with the magnetic field parallel (pink) or perpendicular (black) to the membrane normal

while EPR experiments on the interspin distance in doubly TOAC-labeled analogs in frozen methanol showed that the central portion of the peptide can be structurally heterogeneous.[8]

TABLE 4 Parameters Obtained from the Fitting of the EPR Spectra of [TOAC[4], Lys[6]] TG in Bicelles at *P*:*L* 1:100 and 1:60 and at 308 K: Hyperfine (*A*) Tensor, Diffusion Tensor (*D*), Angles between the Magnetic and the Diffusion Frame (Ω_D), Angle between the Diffusion Frame and the Membrane Normal (Ψ), Order Parameter (*S*).

	^{14}N hyperfine tensor (mT)			Diffusion tensor (MHz)		Ω_D[a]				*S*	
Peptide	A_{xx}	A_{yy}	A_{zz}	$D_{\|\|}$	$D_{\perp}$	α	β	γ	Ψ[b]	***P*:*L* 1:100**	***P*:*L* 1:60**
[TOAC[4], Lys[6]] TG	0.61	0.62	3.11	186	12	0°	20°	90°	0°	0.07	0.04

The *g* tensor is identical to the one in SUV: $g_{xx} = 2.0096$; $g_{yy} = 2.0064$; $g_{zz} = 2.0035$
[a]For an axial diffusion tensor, the angle α is irrelevant.[23]
[b]The error estimate is ~20°.

We prepared three samples of the [TOAC[4], Lys[6]] TG analog at *P*:*L* 1:100, 1:60, and 1:15 ratios. The EPR spectra shown in Figure 5 were collected with the magnetic field parallel (pink) and perpendicular (black) to the membrane normal (*n*) at T=308 K.: the difference between the spectra recorded at the two orientations gives a quick estimate of the degree of order in the bilayer. The spectra of a well-ordered peptide are very different in the two orientations, as previously observed for the two peptaibiotics alamethicin[44] and ampullosporin A.[54] In contrast, the [TOAC[4], Lys[6]] TG analog is not well-ordered in the membrane since its spectra recorded in the two orientations are very similar to each other. In addition, the spectra reveal that a small amount of peptide is not bound to the membrane ($\leq$1%), as shown by the small sharp lines at about 337.5 and 340.5 mT.

To determine the orientation and quantitatively evaluate the order of the peptide (expressed by the order parameter *S*), we performed simulations of the spectra at *P*:*L* 1:100 and 1:60 adopting the same methodology that we previously described in detail.[44] The parameters of the simulation are reported in Table 4. We modeled the peptide motion as a faster diffusion around the main diffusion axis ($D_{||}$), identified as the average helical axis, and a slower diffusion on the axes perpendicular to it ($D_{\perp}$). The set of Euler angles Ω_D defines the orientation of the nitroxide moiety relative to the average helical axis. Ω_D has been estimated from the crystal structure of the TOAC-labeled peptide.[6] The orientation of the average helical axis relative to the membrane normal is defined by the angle Ψ. The orientational order of the peptide in the membrane is quantified by the order parameter *S*. All of the parameters, except for the Ω_D angles, were determined from the spectral fitting.

The diffusion of [TOAC[4], Lys[6]] TG in bicelles is much faster than in SUV, owing to the higher temperature (308 K) at which the experiments were performed. In contrast with the orientation adopted in SUV at a *P*:*L* 1:100 ratio, our simulations suggest that the peptide adopts approximately a transmembrane orientation in bicelles at *P*:*L* 1:100 and 1:60, as derived from the angle $\Psi = 0° \pm 20°$. However, since the order parameter *S* is extremely low ($S = 0.07$–0.04), the peptide orientation is not well-defined. The transmembrane orientation and low-order parameter are in line with the data on perturbation of the order of the phospholipid chains in bicelles by the natural TG.[64] In our previous work,[64] we suggested a transmembrane orientation of the peptide at these two *P*:*L* ratios in tandem with a low order of the helix. POPC SUV and DMPC/DHPC bicelles are characterized by different curvature and membrane thickness (these parameters strongly influence the membrane behavior of peptides). Therefore, the different orientation adopted by the TG analogs at comparable *P*:*L* ratios in SUV and bicelles, already observed for other peptaibiotics, is not surprising.[54,76]

The order parameter of [TOAC[4], Lys[6]] TG is very low, probably owing to the shortness of the TG helix. Longer peptaibiotics display a much higher order parameter than [TOAC[4], Lys[6]] TG: for example, at *P*:*L* 1:100 alamethicin[44] has $S = 0.29$ and 0.47 and ampullosporin A[54] has $S = 0.09$ and 0.165, where these two values refer to the TOAC residue inserted in the more disordered C-terminal part and in the more ordered N-terminal part of the peptide, respectively. The residual order of [TOAC[4], Lys[6]] TG disappears completely at *P*:*L* 1:15. In contrast, a peptide that forms stable transmembrane structures, like alamethicin, keeps a non-zero S even at high *P*:*L*,[44] and only marginally lowers the bilayer order.[64] In conclusion, we suggest that at high (1:15) *P*:*L* ratio the [TOAC[4], Lys[6]]TG analog strongly perturbs the bilayer integrity, thereby hindering the macroscopic orientation of the bicelles and, as a direct consequence, of the membrane-bound peptide as well, as observed for natural TG.[64].

4 | CONCLUSIONS

This study was inspired by the experimental observations that the C-terminal Lol residue and the N-terminal Oct group are both essential for the biological activity of TG and its derivatives,[5,24] but the effects of these moieties on the orientation and dynamics in membranes of these peptides were not known. Therefore, we synthesized several TOAC-labeled TG analogs and determined their membrane dynamics, orientation, and penetration depth by EPR. At a *P*:*L* ratio of 1:100, the TG helix is fully bound to the membrane, lies parallel to the membrane surface, and is inserted below the polar headgroups. The presence of a Lys residue in the mildly

hydrophilic face of the peptide does not affect these parameters. On the contrary, in bicelles at the higher *P*:*L* ratio of 1:60, the peptide adopts a transmembrane orientation. However, this disposition is not as rigid as that exhibited by much longer peptaibiotics (e.g., alamethicin), since the order parameter of TG is extremely low. At even higher peptide concentrations, this parameter vanishes, thus suggesting that TG perturbs bilayer integrity. The nitroxide located on the N-terminal octanoyl chain allowed us to verify its immersion depth. We concluded that the TEMPO-labeled hydrocarbon chain floats towards the bilayer surface. However, this behavior is likely to be affected by the presence of the nitroxide label and might not be fully representative of that of the native octanoyl chain.

In summary, this work allowed us to verify that the overall orientation and insertion in model membranes of the native TG closely resemble those already published for its methyl ester analogs.[7,18] Therefore, reminding that the C-terminal 1,2-amino alcohol is critical for the cytotoxic activity of TG and its derivatives towards eukaryotic cells,[24] our new EPR data on different analogs suggest that this alcoholic function probably affects binding affinity, and/or partakes in a specific interaction with eukaryotic cells, rather than influencing peptide orientation in the membrane.

REFERENCES

[1] C. Toniolo, H. Brückner, *Peptaibiotics: Fungal Peptides Containing α-Dialkyl α-Amino Acids, Wiley-VCH, Weinheim, Germany* ***2009***.

[2] B. Leitgeb, A. Szekeres, L. Manczinger, C. Vagvolgyi, L. Kredics, *Chem. Biodivers.* **2007**, *4*, 1027.

[3] C. Auvin-Guette, S. Rebuffat, Y. Prigent, B. Bodo, *J. Am. Chem. Soc.* **1992**, *114*, 2170.

[4] C. Toniolo, C. Peggion, M. Crisma, F. Formaggio, X. Q. Shui, D. S. Eggleston, *Nat. Struct. Biol.* **1994**, *1*, 908.

[5] C. Toniolo, M. Crisma, F. Formaggio, C. Peggion, V. Monaco, C. Goulard, S. Rebuffat, B. Bodo, *J. Am. Chem. Soc.* **1996**, *118*, 4952.

[6] V. Monaco, F. Formaggio, M. Crisma, C. Toniolo, P. Hanson, G. Millhauser, C. George, J. R. Deschamps, J. L. Flippen-Anderson, *Bioorg. Med. Chem.* **1999**, *7*, 119.

[7] V. Monaco, F. Formaggio, M. Crisma, C. Toniolo, P. Hanson, G. L. Millhauser, *Biopolymers* **1999**, *50*, 239.

[8] D. J. Anderson, P. Hanson, J. McNulty, G. Millhauser, V. Monaco, F. Formaggio, M. Crisma, C. Toniolo, *J. Am. Chem. Soc.* **1999**, *121*, 6919.

[9] A. D. Milov, Y. D. Tsvetkov, F. Formaggio, M. Crisma, C. Toniolo, J. Raap, *J. Am. Chem. Soc.* **2000**, *122*, 3843.

[10] A. D. Milov, Y. D. Tsvetkov, F. Formaggio, M. Crisma, C. Toniolo, G. L. Millhauser, J. Raap, *J. Phys. Chem. B* **2001**, *105*, 11206.

[11] A. D. Milov, Y. D. Tsvetkov, F. Formaggio, M. Crisma, C. Toniolo, J. Raap, *J. Am. Chem. Soc.* **2001**, *123*, 3784.

[12] C. Toniolo, M. Crisma, F. Formaggio, C. Peggion, R. F. Epand, R. M. Epand, *Cell. Mol. Life Sci.* **2001**, *58*, 1179.

[13] C. Peggion, F. Formaggio, M. Crisma, R. F. Epand, R. M. Epand, C. Toniolo, *J. Pept. Sci.* **2003**, *9*, 679.

[14] A. D. Milov, R. I. Samoilova, Y. D. Tsvetkov, V. A. Gusev, F. Formaggio, M. Crisma, C. Toniolo, J. Raap, *Appl. Magn. Reson.* **2002**, *23*, 81.

[15] A. D. Milov, Y. D. Tsvetkov, F. Formaggio, M. Crisma, C. Toniolo, J. Raap, *J. Pept. Sci.* **2003**, *9*, 690.

[16] A. D. Milov, D. A. Erilov, E. S. Salnikov, Y. D. Tsvetkov, F. Formaggio, C. Toniolo, *J. Raap, Phys. Chem. Chem. Phys.* **2005**, *7*, 1794.

[17] A. D. Milov, R. I. Samoilova, Y. D. Tsvetkov, F. Formaggio, C. Toniolo, J. Raap, *Appl. Magn. Reson.* **2005**, *29*, 703.

[18] E. S. Salnikov, D. A. Erilov, A. D. Milov, Y. D. Tsvetkov, C. Peggion, F. Formaggio, C. Toniolo, J. Raap, S. A. Dzuba, *Biophys. J.* **2006**, *91*, 1532.

[19] M. De Zotti, B. Biondi, F. Formaggio, C. Toniolo, L. Stella, Y. Park, K. S. Hahm, *J. Pept. Sci.* **2009**, *15*, 615.

[20] M. De Zotti, B. Biondi, C. Peggion, F. Formaggio, Y. Park, K. S. Hahm, C. Toniolo, *Org. Biomol. Chem.* **2012**, *10*, 1285.

[21] M. De Zotti, B. Biondi, Y. Park, K. S. Hahm, M. Crisma, C. Toniolo, F. Formaggio, *Amino Acids* **2012**, *43*, 1761.

[22] S. Bobone, Y. Gerelli, M. De Zotti, G. Bocchinfuso, A. Farrotti, B. Orioni, F. Sebastiani, E. Latter, J. Penfold, R. Senesi, F. Formaggio, A. Palleschi, C. Toniolo, G. Fragneto, L. Stella, *Biochim. Biophys. Acta (Biomembr.)* **2013**, *1828*, 1013.

[23] C. Peggion, B. Biondi, C. Battistella, M. De Zotti, S. Oancea, F. Formaggio, C. Toniolo, *Chem. Biodivers.* **2013**, *10*, 904.

[24] R. Tavano, G. Malachin, M. De Zotti, C. Peggion, B. Biondi, F. Formaggio, E. Papini, *Biochim. Biophys. Acta (Biomembr.)* **2015**, *1848*, 134.

[25] R. F. Epand, R. M. Epand, F. Formaggio, M. Crisma, H. Wu, R. I. Lehrer, C. Toniolo, *Eur. J. Biochem.* **2001**, *268*, 703.

[26] C. Heuber, F. Formaggio, C. Baldini, C. Toniolo, K. Müller, *Chem. Biodivers.* **2007**, *4*, 1200.

[27] C. Peggion, B. Biondi, M. De Zotti, S. Oancea, F. Formaggio, C. Toniolo, *J. Pept. Sci.* **2013**, *19*, 246.

[28] V. Monaco, E. Locardi, F. Formaggio, M. Crisma, S. Mammi, E. Peggion, C. Toniolo, S. Rebuffat, B. Bodo, *J. Pept. Res.* **1998**, *52*, 261.

[29] E. Locardi, S. Mammi, E. Peggion, V. Monaco, F. Formaggio, M. Crisma, C. Toniolo, B. Bodo, S. Rebuffat, J. Kamphuis, Q. B. Broxterman, *J. Pept. Sci.***1998**, *4*, 389.

[30] M. De Zotti, S. Bobone, A. Bortolotti, E. Longo, B. Biondi, C. Peggion, F. Formaggio, C. Toniolo, A. Dalla Bona, B. Kaptein, L. Stella, *Chem. Biodivers.***2015**, *12*, 513.

[31] M. Venanzi, E. Gatto, G. Bocchinfuso, A. Palleschi, L. Stella, F. Formaggio, C. Toniolo, *ChemBioChem* **2006**, *7*, 43.

[32] L. Stella, C. Mazzuca, M. Venanzi, A. Palleschi, M. Didoné, F. Formaggio, C. Toniolo, B. Pispisa, *Biophys. J.* **2004**, *86*, 936.

[33] E. Gatto, C. Mazzuca, L. Stella, M. Venanzi, C. Toniolo, B. Pispisa, *J. Phys. Chem. B* **2006**, *110*, 22813.

[34] G. Bocchinfuso, A. Palleschi, B. Orioni, G. Grande, F. Formaggio, C. Toniolo, Y. Park, K. S. Hahm, L. Stella, *J. Pept. Sci.* **2009**, *15*, 550.

[35] C. Mazzuca, L. Stella, M. Venanzi, F. Formaggio, C. Toniolo, B. Pispisa, *Biophys. J.* **2005**, *88*, 3411.

[36] M. Venanzi, E. Gatto, G. Bocchinfuso, A. Palleschi, L. Stella, C. Baldini, F. Formaggio, C. Toniolo, *J. Phys. Chem. B* **2006**, *110*, 22834.

[37] C. Mazzuca, B. Orioni, M. Coletta, F. Formaggio, C. Toniolo, G. Maulucci, M. De Spirito, B. Pispisa, M. Venanzi, L. Stella, *Biophys. J.* **2010**, *99*, 1791.

[38] S. Iftemi, M. De Zotti, F. Formaggio, C. Toniolo, L. Stella, T. Luchian, *Chem. Biodivers.* **2014**, *11*, 1069.

[39] L. J.Berliner, *Spin Labeling the Next Millennium, Plenum Press, New York* ***1998***.

[40] Z. Y. J. Sun, Y. Cheng, M. Kim, L. Song, J. Choi, U. J. Kudahl, V. Brusic, B. Chowdhury, L. Yu, M. S. Seaman, G. Bellot, W. M. Shih, G. Wagner, E. L. Reinherz, *J. Mol. Biol.* **2014**, *426*, 1095.

[41] C. Altenbach, D. A. Greenhalgh, H. G. Khorana, W. L. Hubbell, *Proc. Natl. Acad. Sci. USA* **1994**, *91*, 1667.

[42] D. J. Mayo, J. J. Inbaraj, N. Subbaraman, S. M. Grosser, C. A. Chan, G. A. Lorigan, *J. Am. Chem. Soc.* **2008**, *130*, 9656.

[43] M. Bortolus, G. Parisio, A. L. Maniero, A. Ferrarini, *Langmuir* **2011**, *27*, 12560.

[44] M. Bortolus, M. De Zotti, F. Formaggio, A. L. Maniero, *Biochim. Biophys. Acta (Biomembr.)* **2013**, *1828*, 2620.

[45] T. B. Cardon, E. K. Tiburu, G. A. Lorigan, *J. Magn. Reson.* **2003**, *161*, 77.

[46] U. H. N. Durr, R. Soong, A. Ramamoorthy, *Prog. Nucl. Magn. Reson.* **2013**, *69*, 1.

[47] R. Marchetto, S. Schreier, C. R. Nakaie, *J. Am. Chem. Soc.* **1993**, *115*, 11042.

[48] C. Toniolo, M. Crisma, F. Formaggio, *Biopolymers* **1998**, *47*, 153.

[49] S. Schreier, J. Bozelli, Jr., N. Marín, R. F. Vieira, C. Nakaie, *Biophys. Rev.* **2012**, *4*, 45.

[50] A. Dalzini, C. Bergamini, B. Biondi, M. De Zotti, G. Panighel, R. Fato, C. Peggion, M. Bortolus, A. L. Maniero, *Sci. Rep.* **2016**, *6*, 24000.

[51] G. Mobbili, E. Crucianelli, A. Barbon, M. Marcaccio, M. Pisani, A. Dalzini, E. Ussano, M. Bortolus, P. Stipa, P. Astolfi, *RSC Adv.* **2015**, *5*, 98955.

[52] C. S. Klug, W. Y. Su, J. B. Feix, *Biochemistry* **1997**, *36*, 13027.

[53] L. A. Dalton, J. O. McIntyre, S. Fleischer, *Biochemistry* **1987**, *26*, 2117.

[54] M. Bortolus, A. Dalzini, F. Formaggio, C. Toniolo, M. Gobbo, A. L. Maniero, *Phys. Chem. Chem. Phys.* **2016**, *18*, 749.

[55] M. P. Nieh, C. J. Glinka, S. Krueger, R. S. Prosser, J. Katsaras, *Langmuir* **2001**, *17*, 2629.

[56] D. E. Budil, S. Lee, S. Saxena, J. H. Freed, *J. Magn. Reson. A* **1996**, *120*, 155.

[57] Z. C. Liang, Y. Lou, J. H. Freed, L. Columbus, W. L. Hubbell, *J. Phys. Chem. B* **2004**, *108*, 17649.

[58] B. M. Kroncke, P. S. Horanyi, L. Columbus, *Biochemistry* **2010**, *49*, 10045.

[59] J. J. Inbaraj, T. B. Cardon, M. Laryukhin, S. M. Grosser, G. A. Lorigan, *J. Am. Chem. Soc.* **2006**, *128*, 9549.

[60] D. Xu, R. H. Crepeau, C. K. Ober, J. H. Freed, *J. Phys. Chem.* **1996**, *100*, 15873.

[61] L. Hoffman, R. A. Stein, R. J. Colbran, H. S. Mchaourab, *EMBO J* **2011**, *30*, 1251.

[62] J. P. Barnes, Z. C. Liang, H. S. Mchaourab, J. H. Freed, W. L. Hubbell, *Biophys. J.* **1999**, *76*, 3298.

[63] M. Bortolus, P. Centomo, M. Zecca, A. Sassi, K. Jerabek, A. L. Maniero, B. Corain, *Chem. Eur. J.* **2012**, *18*, 4706.

[64] M. Bortolus, A. Dalzini, C. Toniolo, K. S. Hahm, A. L. Maniero, *J. Pept. Sci.***2014**, *20*, 517.

[65] D. Kurad, G. Jeschke, D. Marsh, *Appl. Magn. Reson.* **2001**, *21*, 469.

[66] M. C. Manning, R. W. Woody, *Biopolymers* **1991**, *31*, 569.

[67] C. Toniolo, F. Formaggio, R. W. Woody, in *Comprehensive Chiroptical Spectroscopy, Vol.* 2 *(Eds: N. Berova, P. L. Polavarapu, K. Nakanishi, R. W.. Woody), Wiley, New York* ***2012****, 499.*

[68] C. Toniolo, A. Polese, F. Formaggio, M. Crisma, J. Kamphuis, *J. Am. Chem. Soc.* **1996**, *118*, 2744.

[69] F. Formaggio, M. Crisma, P. Rossi, P. Scrimin, B. Kaptein, Q. B. Broxterman, J. Kamphuis, C. Toniolo, *Chem. Eur. J.* **2000**, *6*, 4498.

[70] D. Eisenberg, *Annu. Rev. Biochem.* **1984**, *53*, 595.

[71] A. Tossi, L. Sandri, A. Giangaspero, *Biopolymers (Pept. Sci.)* **2000**, *55*, 4.

[72] A.Tossi, L. Sandri, A. Giangaspero, in *Peptides (Eds: E. Benedetti, C. Pedone), Edizioni Ziino, Sorrento, Italy* ***2002****, 416.*

[73] Z. Liang, J. H. Freed, R. S. Keyes, A. M. Bobst, *J. Phys. Chem. B* **2000**, *104*, 5372.

[74] S. A. Goldman, G. V. Bruno, J. H. Freed, *J. Phys. Chem.* **1972**, *76*, 1858.

[75] N. Kucerka, M. P. Nieh, J. Katsaras, *Biochim. Biophys. Acta (Biomembr.)* **2011**, *1808*, 2761.

[76] D. Marsh, M. Jost, C. Peggion, C. Toniolo, *Biophys. J.* **2007**, *92*, 4002.

How to cite this article: Bortolus M, Dalzini A, Lisa Maniero A, Panighel G, Siano A, Toniolo C, De Zotti M, and Formaggio F. Insights into peptide-membrane interactions of newly synthesized, nitroxide-containing analogs of the peptaibiotic trichogin GA IV using EPR. *Peptide Science* 2017;108:e22913. https://doi.org/10.1002/bip.22913